

Active Anomaly Detection for time-domain discoveries

E. E. O. Ishida^{1*}, M. V. Kornilov^{2,3†}, K. L. Malanchev^{2,3}, M. V. Pruzhinskaya², A. A. Volnova⁴, V. S. Korolev^{5,6}, F. Mondon¹, S. Sreejith¹, A. Malancheva⁷ and S. Das⁸

¹ *Université Clermont Auvergne, CNRS/IN2P3, LPC, F-63000 Clermont-Ferrand, France*

² *Lomonosov Moscow State University, Sternberg Astronomical Institute, Universitetsky pr. 13, Moscow, 119234, Russia*

³ *National Research University Higher School of Economics, 21/4 Staraya Basmannaya Ulitsa, Moscow, 105066, Russia*

⁴ *Space Research Institute of the Russian Academy of Sciences (IKI), 84/32 Profsoyuznaya Street, Moscow, 117997, Russia*

⁵ *Central Aerohydrodynamic Institute, 1 Zhukovsky st, Zhukovsky, Moscow Region, 140180, Russia*

⁶ *Moscow Institute of Physics and Technology, 9 Institutskiy per., Dolgoprudny, Moscow Region, 141701, Russia*

⁷ *Independent researcher*

⁸ *Washington State University, Pullman, WA 99163, USA*

Accepted XXX. Received YYY; in original form ZZZ

ABSTRACT

We present the first application of adaptive machine learning to the identification of anomalies in a data set of non-periodic astronomical light curves. The method follows an active learning strategy where highly informative objects are selected to be labelled. This new information is subsequently used to improve the machine learning model, allowing its accuracy to evolve with the addition of every new classification. For the case of anomaly detection, the algorithm aims to maximize the number of real anomalies presented to the expert by slightly modifying the decision boundary of a traditional isolation forest in each iteration. As a proof of concept, we apply the Active Anomaly Discovery (AAD) algorithm to light curves from the Open Supernova Catalog and compare its results to those of a static Isolation Forest (IF). For both methods, we visually inspected objects within 2% highest anomaly scores. We show that AAD was able to identify $\sim 80\%$ more true anomalies than IF. This result is the first evidence that AAD algorithms can play a central role in the search for new physics in the era of large scale sky surveys.

Key words: methods: data analysis – supernovae: general – stars: variables: general

1 INTRODUCTION

The detection of new astronomical sources is one of the most anticipated outcomes from the next generation of large scale sky surveys. Experiments like the Large Synoptic Survey Telescope¹ (LSST) are expected to continuously monitor large areas of the sky with unprecedented scrutiny, certainly leading to the detection of unforeseen astrophysical phenomena. At the same time, the volume of data gathered every night will also increase to unprecedented levels, rendering serendipitous discoveries unlikely. In the era of big data, most detected sources will never be visually inspected, and the use of automated algorithms is unavoidable.

Although being relatively new in the astronomical scenario, the task of automatically identifying peculiar objects

within a large set of normal instances has been highly explored in many areas of research (Aggarwal 2016). This led to the development of a number of machine learning (ML) algorithms for anomaly detection (AD) with a large range of applications (Mehrotra et al. 2017). In astronomy, these techniques have been largely applied to areas like the identification of anomalous galaxy spectra (Baron & Poznanski 2017), problematic objects in photometric redshift estimation tasks (Hoyle et al. 2015), light curves of transients (Zhang & Zou 2018; Pruzhinskaya et al. 2019) and variable stars (e.g., Rebbapragada et al. 2009; Nun et al. 2014; Giles & Walkowicz 2019), among others.

Despite encouraging results, the application of traditional AD algorithms to the astronomical scenario is far from trivial. Most of these strategies consist of constructing a statistical model for the nominal data and identifying as anomalous objects which highly deviate from this description. These sources necessarily go through further scrutiny by an expert which confirms (or not) the discovery of a new

* E-mail: emille.ishida@clermont.in2p3.fr (EEOI)

† E-mail: matwey@sai.msu.ru

¹ <https://www.lsst.org/>

phenomena. However, frequently a statistical anomaly may be a result of observational defects or other spurious interference which are not scientifically interesting — leading to a high rate of false positives and a proportional fraction of resources, and research time, spent to further investigate non-peculiar objects.

Taking into account that measuring details of a new source often requires the allocation of spectroscopic follow-up resources, the development of anomaly detection strategies able to deliver a low rate of false positives is paramount. Specially in the light of the upcoming generation of telescopes, which will drastically increase the volume of nominal data and, in the process, pose a challenging anomaly detection task. In machine learning jargon, we look for an adaptive recommendation system which must be able to optimally exploit a given ML model by carefully choosing the construction of the training sample.

Active learning (AL) is a subclass of ML algorithms designed to guide an optimal allocation of labelling resources in situations where labels are expensive and/or time consuming. In the context of large scale photometric surveys, this translates into a recommendation system for planning on the distribution of follow-up resources — given a particular scientific goal. Prototypes using this underlying philosophy for supervised learning tasks were applied to the determination of stellar population parameters (Solorio et al. 2005), supervised classification of variable stars (Richards et al. 2012) and microlensing events (Xia et al. 2016), photometric redshift estimation (Vilalta et al. 2017), supernova photometric classification (Ishida et al. 2019) and determination of galaxy morphology (Walmsley et al. 2019).

In this work, we present the first application of AL for anomaly detection in astronomical data. As a proof of concept, we applied the active anomaly detection strategy proposed by Das et al. (2017) in the search for peculiar light curves within the Open Supernova Catalog (Guillochon et al. 2017). Used in combination with a traditional isolation forest (IF) algorithm, the method allows increasingly larger incidence of true positives among objects presented to the expert — enabling a better allocation of resources with the evolution of a given survey.

In what follows, we present the data and preprocessing analysis in Section 2. In Section 3 we describe the AAD algorithm and corresponding results are presented in Section 4. Finally, we present our conclusions and discuss implications for future large scale astronomical surveys in Section 5.

2 DATA

We used data from the Open Supernova Catalog (Guillochon et al. 2017). This is a public repository containing supernova light curves, spectra and meta data from a large range of different sources. It is known to also hold a small percentage of non-supernovae contaminants — which makes it well suited for our goal.

Following basic quality cuts, light curves originally observed in *BRI* filters were converted to *gri*² and the entire

set was submitted to a MULTIVARIATE GAUSSIAN PROCESS³ pipeline. This procedure resulted in smoothed light curves which can be homogeneously sampled in time. Details on data selection and pre-processing pipeline are described in Pruzhinskaya et al. (2019).

Our final data matrix consists of 1999 objects (lines) with 374 features (columns). The feature set includes the log-likelihood from the Gaussian process approximation, the light curve maximum flux and 121 normalised photometric points per filter (this corresponds to a grid of $[-20, +100]$ days since maximum brightness with 1-day interval) concatenated according to their effective wavelength.

3 METHODOLOGY

In order to enable the comparison of active anomaly detection results with those obtained with traditional AD and with a blind search, we visually inspected instances within 2% highest anomaly scores (40 objects) according to 3 different strategies: random sampling (RS), isolation forest (Section 3.1) and active anomaly detection (Section 3.2). This manual screening allowed us to coherently estimate the rate of true positives for all strategies. Each candidate was considered anomalous or nominal according to the guidelines described in Section 3.3 and the expert was allowed to consult external literature to make a decision on controversial samples.

3.1 Isolation forest

Isolation forest is a tree-based ensemble⁴ method first proposed by Liu et al. (2008). It considers anomalies as data instances which are isolated from normal samples in a given parameter space. In this context, anomalies are identified as objects with the smallest path length between the root and an external node in a randomised decision tree. The combination of results from a number of trees built with different sub-samples makes it robust to overfitting. By exploiting the fact that anomalies are, by definition, rare and prone to isolation, the method avoids the need of expensive distance calculations or statistical modelling of the normal instances.

3.2 Active Anomaly Detection

AL algorithms allow atoms of expert feedback to be incorporated into the learning model and, consequently, improve the accuracy of the predicted results. As such, they work in conjunction with a traditional ML strategy which must either be sensitive to small changes in input information or allow the incorporation of such knowledge in subsequent fine tuning of the model. Decision trees fulfil these requirements (see e.g., Loh 2014). Moreover, for the specific case of AL for AD tasks, ensemble methods are specially interesting.

Ensemble methods for AD rely on the assumption that true anomalies will have a high anomaly score across the entire ensemble, while nominal samples will be assigned lower

² <http://www.sdss3.org/dr8/algorithms/sdssUBVRITransform.php>

³ <https://github.com/matwey/gp-multistate-kernel>

⁴ Those which use a collection classifiers in the construction of the final prediction.

ones — despite values of the scores themselves being different among members. This allows us to define a weight vector \mathbf{w} , where each element denotes the impact of a given member of the ensemble in the final anomaly score. In the case of N members with perfect predictions, this will be a uniform vector, $w_i = 1/\sqrt{N}$ for $i \in [1, N]$. In a more realistic scenario, certain members will be better predictors than others and we can translate this behaviour by assigning larger weights to more accurate predictors and lower ones to noisier members of the ensemble (see Figure 1 of Das et al. 2018).

Active Anomaly Discovery (an active anomaly detection algorithm proposed by Das et al. 2017, hereafter AAD) exploits this adaptability in order to fine tune the ensemble according to a specific definition of anomaly, as pointed by the expert through a series of real examples. The algorithm starts by training a traditional IF and presenting the candidate with highest anomaly score to be classified. If the expert judges the candidate to be a real anomaly the state of the model does not change and the next highest scored candidate is presented. Whenever a given candidate is classified as a false positive, the model is updated through a re-scaling of the anomaly scores (changes in \mathbf{w}). This slight modification preserves the structure of the original forest while adapting the importance weights to ensure that labelled anomalies are assigned higher anomaly scores than labelled normal instances. Further details about the algorithm is given in Appendix A and in Das et al. (2017, 2018).

3.3 Defining anomalies

The definition of anomaly strongly depends on the researcher goals and objectives. In this work, we are mainly interested in identifying non-supernovae contamination and/or supernovae with unusual properties (Milisavljevic & Margutti 2018) within the Open Supernova Catalog. Non-supernovae objects can be divided in cases of misclassification (quasars, binary microlensing events, novae, etc.), completely new classes of objects or sources observed under extreme conditions. We did not consider anomalous cases of possible misclassifications due to a signal which is too small to allow a confident conclusion regarding the nature of the transient. These cases can not be carefully studied due to low signal to noise ratio and, therefore, are not astrophysically interesting.

As unusual supernovae we consider objects that were proved to be peculiar by previous studies. This could be any kind of peculiarities: the signature of interaction with interstellar medium, unusual rise or decline light curve rate or any other features which are not representative of the corresponding supernova type. We also consider as anomalies 91T-like and 91bg-like Type Ia supernovae since their contamination in cosmological samples of supernovae can affect the measurements of cosmological parameters. This is extremely important for large surveys like LSST, which aims to constrain cosmological parameters using the bulk of normal type Ia SNe. All non-physical effects, e.g. artefacts of interpolation, were not considered as anomalies.

The above criteria were designed to serve as an example of the kind of requirements one might impose to the AAD algorithm. These will certainly vary depending on the research goal, available labelling resources and data at hand. However, for the purposes of this work, the exact anomaly

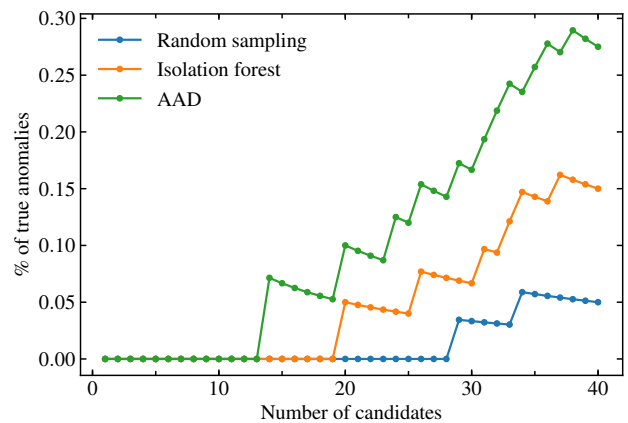


Figure 1. Fraction of true anomalies as a function of the total number of candidates scrutinised by the expert. The plot shows results obtained with random sampling (blue), isolation forest (orange) and active anomaly discovery (green) algorithms.

definition serves merely to illustrate the flexibility of our framework. The global behaviour of exercises using different anomaly criteria should resemble those presented in Section 4.

4 RESULTS

Figure 1 shows how the percentage of true anomalies behaves as a function of the total number of objects inspected by the expert. The figure was constructed considering objects in order of decreasing anomaly score (for isolation forest) and following the order in which they were presented as candidates (for AAD and RS). RS achieved a maximum true positive rate of 5%. IF was able to boost this to 15% while AAD identified 27% true positives. This represents an increase of 80% in the number of true anomalies detected for the same amount of resources spent in scrutinising candidates. Moreover, although both strategies require a *burn-in* period to start identifying interesting sources, AAD presents the first anomaly much earlier (14th) than in the case of IF (20th).

A more detailed comparison between IF and AAD results is displayed in Figure 2 (full list of identified anomalies is given in Appendix B). The diagram shows the identification of all objects presented as anomaly candidates by IF (top) and AAD (bottom). The first two objects selected as outliers are the same for both algorithms, with a discrepancy only starting from the third one. The detected anomalies are ordered by score in the case of IF. For AAD they represent the highest anomaly score for successive iterations of the active learning loop. True anomalies are highlighted in yellow. The plot clearly illustrates not only the higher incidence of true anomalies for AAD vs IF (11 vs 6), but also the larger density among latter candidates. The lines connecting objects present in both branches show that the first half of the list contain many objects in common between the two algorithms. On the other hand, the second half of the AAD list encloses true anomalies which are absent in the upper branch. This demonstrates that the algorithm is able to adapt to the definition of anomaly according to the

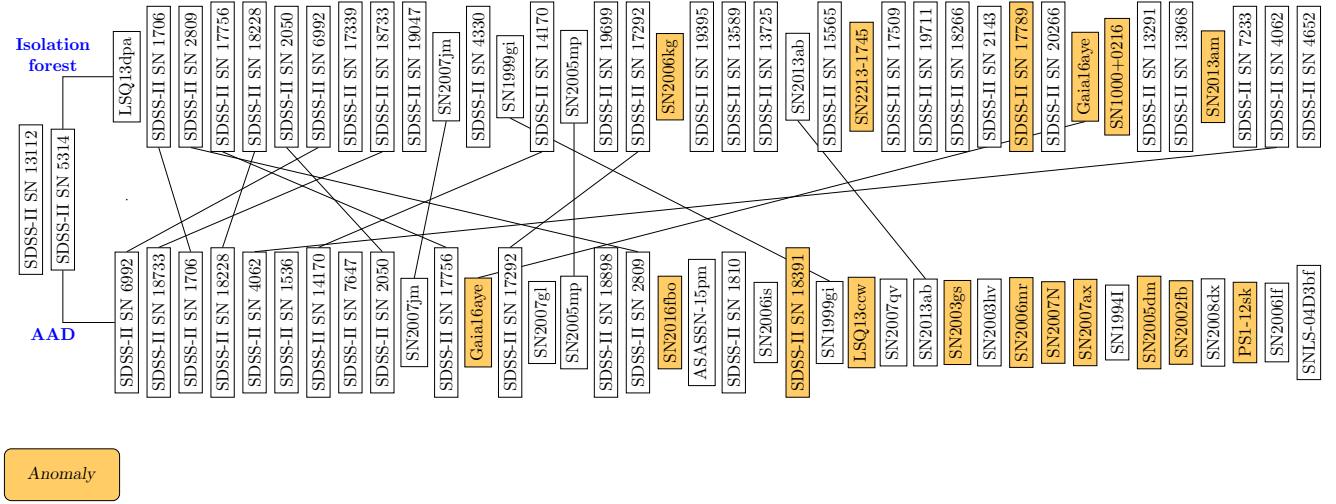


Figure 2. Comparison between the outputs of the isolation forest and active anomaly discovery (AAD) algorithms. Rectangles contain object names selected as the outliers in order of importance. The yellow boxes show anomalies visually confirmed. Solid lines indicate the objects which are in common in both branches.

feedback received from the expert. Moreover, one of the most obvious peculiar objects in our sample is a binary microlensing event, Gaia16aye (see Appendix C). It was assigned the 33rd highest anomaly score by isolation forest, while being the first real anomaly presented by AAD — in the 14th iteration. These results are the first evidence that adaptive learning algorithms can be important tools in planning optimised distribution of resources in the search for peculiar astronomical objects.

5 CONCLUSIONS

The next generation of large scale sky surveys will certainly detect a variety of new astrophysical sources. However, since every photometrically observed candidate requires further investigation via spectroscopic observations, the development of automated anomaly detection algorithms with low incidence of false positives is crucial. Moreover, such algorithms must be able to detect scientifically interesting anomalies — as oppose to spurious features due to observing conditions or errors in the data processing pipeline. Active learning methods are known to perform well in such data scenarios. They represent a class of adaptive learning strategies where expert feedback is sequentially incorporated into the machine learning model to allow high accuracy in predictions while maintaining the distribution of analysis resources under control.

We report results supporting the use of active learning algorithms in the allocation of resources for astronomical discovery. We use light curves from the Open Supernova Catalog as a test bench to compare the rate of true anomalies discovered by a traditional isolation forest algorithm to those identified by active anomaly detection (Das et al. 2017). We show that active anomaly detection is able to increase the incidence of true anomalies in 80% when compared to the static isolation forest. Moreover, the algorithm can adapt

the definition of anomaly imposed by the expert — which leads to a higher density of true positives in latter iterations. This ensures not only a larger number of peculiar objects in total, but also guarantees that each new scrutinised source will, in the long run, contribute to the improvement of the learning model. In this context, not even the resources spent in analysing false positives, in the beginning of the survey, are wasted.

In order to ensure a reliable estimation of true positive rates, we presented a simplified scenario enclosing ~ 2000 objects. This allowed visual confirmation of all objects within 2% highest anomaly scores for all algorithms. We acknowledge that important issues need to be further addressed (e.g. the variability of results for different feature extraction methods, stream mode learning and scalability). Nevertheless, results presented here support the hypothesis that adaptive techniques can play important roles in the future of astronomy.

ACKNOWLEDGEMENTS

E. E. O. Ishida and S. Sreejith acknowledge support from CNRS 2017 MOMENTUM grant under project *Active Learning for Large Scale Sky Surveys*. M. Pruzhinskaya and M. Kornilov are supported by RFBR grant according to the research project 18-32-00426 for anomaly analysis and LCs approximation. K. Malanchev is supported by RFBR grant 18-32-00553 for preparing the Open Supernova Catalog data. A. Volnova acknowledges support from RSF grant 18-12-00522 for analysis of interpolated LCs. We used the equipment funded by the Lomonosov Moscow State University Program of Development. The authors acknowledge the support from the Program of Development of M.V. Lomonosov Moscow State University (Leading Scientific School “Physics of stars, relativistic objects and galaxies”). This research has made use of NASA’s Astrophysics Data System Biblio-

graphic Services and following PYTHON software packages: NUMPY (van der Walt et al. 2011), MATPLOTLIB (Hunter 2007), SCIPY (Jones et al. 2001), PANDAS (McKinney 2010), and SCIKIT-LEARN (Pedregosa et al. 2011).

REFERENCES

- Aggarwal C., 2016, Outlier Analysis. Springer International Publishing, <https://books.google.fr/books?id=KyG1DQAAQBAJ>
- Aldering G., et al., 2005, The Astronomer’s Telegram, 596, 1
- Bakis V., et al., 2016, The Astronomer’s Telegram, 9376
- Baron D., Poznanski D., 2017, MNRAS, 465, 4530
- Bassett B., et al., 2006, Central Bureau Electronic Telegrams, 688, 1
- Blondin S., et al., 2012, AJ, 143, 126
- Contreras C., et al., 2010, AJ, 139, 519
- Cooke J., et al., 2012, Nature, 491, 228
- Das S., Wong W.-K., Fern A., Dietterich T. G., Amran Siddiqui M., 2017, arXiv e-prints, p. arXiv:1708.09441
- Das S., Rakibul Islam M., Kannappan Jayakodi N., Rao Doppa J., 2018, arXiv e-prints, p. arXiv:1809.06477
- Folatelli G., et al., 2013, ApJ, 773, 53
- Foley R. J., et al., 2018, MNRAS, 475, 193
- Giles D., Walkowicz L., 2019, MNRAS, 484, 834
- González-Gaitán S., et al., 2014, ApJ, 795, 142
- Guillochon J., Parrent J., Kelley L. Z., Margutti R., 2017, ApJ, 835, 64
- Hoyle B., Rau M. M., Paech K., Bonnett C., Seitz S., Weller J., 2015, MNRAS, 452, 4183
- Hunter J. D., 2007, Computing in Science and Engineering, 9, 90
- Ishida E. E. O., et al., 2019, MNRAS, 483, 2
- Jones E., Oliphant T., Peterson P., et al., 2001, SciPy: Open source scientific tools for Python, <http://www.scipy.org/>
- Krisciunas K., et al., 2009, AJ, 138, 1584
- Lisakov S. M., Dessart L., Hillier D. J., Waldman R., Livne E., 2018, MNRAS, 473, 3863
- Liu F. T., Ting K. M., Zhou Z.-H., 2008, in 2008 Eighth IEEE International Conference on Data Mining. pp 413–422
- Loh W.-Y., 2014, International Statistical Review, 82, 329
- McKinney W., 2010, in van der Walt S., Millman J., eds, Proceedings of the 9th Python in Science Conference. pp 51 – 56
- Mehrotra K. G., Mohan C. K., Huang H., 2017, Anomaly Detection Principles and Algorithms, 1st edn. Springer Publishing Company, Incorporated
- Milislavljevic D., Margutti R., 2018, Space Sci. Rev., 214, 68
- Nakano S., et al., 2013, Central Bureau Electronic Telegrams, 3440
- Nun I., Pichara K., Protopapas P., Kim D.-W., 2014, ApJ, 793, 23
- Östman L., et al., 2011, A&A, 526, A28
- Pastorello A., et al., 2015, MNRAS, 449, 1954
- Pedregosa F., et al., 2011, Journal of Machine Learning Research, 12, 2825
- Pruzhinskaya M. V., Malanchev K. L., Kornilov M. V., Ishida E. E. O., Mondon F., Volnova A. A., Korolev V. S., 2019, Monthly Notices of the Royal Astronomical Society, 489, 3591
- Rebbapragada U., Protopapas P., Brodley C. E., Alcock C., 2009, arXiv e-prints, p. arXiv:0905.3428
- Richards J. W., et al., 2012, ApJ, 744, 192
- Sako M., et al., 2018, PASP, 130, 064002
- Sanders N. E., et al., 2013, ApJ, 769, 39
- Solorio T., Fuentes O., Terlevich R., Terlevich E., 2005, MNRAS, 363, 543
- Stritzinger M. D., et al., 2011, AJ, 142, 156
- Vilalta R., Ishida E. E. O., Beck R., Sutrisno R., de Souza R. S., Mahabal A., 2017, in 2017 IEEE Symposium Series on Computational Intelligence (SSCI).
- Walmsley M., et al., 2019, arXiv e-prints, p. arXiv:1905.07424
- Wyrzykowski L., et al., 2016, The Astronomer’s Telegram, 9507
- Xia X., Protopapas P., Doshi-Velez F., 2016, Cost-Sensitive Batch Mode Active Learning: Designing Astronomical Observation by Optimizing Telescope Time and Telescope Choice. pp 477–485, doi:10.1137/1.9781611974348.54
- Zhang R., Zou Q., 2018, Journal of Physics: Conference Series, 1061, 012012
- van der Walt S., Colbert S. C., Varoquaux G., 2011, Computing in Science and Engineering, 13, 22

APPENDIX A: ACTIVE ANOMALY DETECTION ALGORITHM

We give below a brief description on how the weights are updated in each iteration of the learning loop. For further details see Das et al. (2017, 2018).

The algorithm starts by training a traditional isolation forest (Liu et al. 2008), which requires the user to determine a contamination level, $\tau \in [0, 1]$, a percentile used to separate normal objects from anomalies. Once the forest is trained, we denote q_τ the anomaly score corresponding to the chosen contamination level. Each *leaf node* in the forest is subsequently assigned an uniform weight, $w_i = 1/\sqrt{N_{\text{nodes}}}$. Supposing the average number of leaf nodes per tree is N_{avt} , the dimension of the weight vector will be equal to the total number of nodes, $\dim(\mathbf{w}) = N_{\text{trees}} \times N_{\text{avt}} = N_{\text{nodes}}$. We will also define a vector \mathbf{z} for each object in the data set which also has dimension N_{nodes} . Considering the entire set of leaf nodes as a spatial parameter space, each element of \mathbf{z} marks the final positions occupied by a given object throughout the forest. In this context, for each object, \mathbf{z} is sparse vector with 0 in all elements corresponding to leaf nodes not occupied. We shall denote the anomaly score of the i -th object as $q_i = \mathbf{z}_i \cdot \mathbf{w}$.

Given a data set \mathbf{H} , we call $\mathbf{H}_F \subseteq \mathbf{H}$ the subset of objects that were already analyzed by the expert, $\mathbf{H}_A \subseteq \mathbf{H}_F$ the set of labelled anomalies and $\mathbf{H}_N \subseteq \mathbf{H}_F$ the set of labelled normal objects. Let $y_i \in [\text{anomaly}, \text{normal}]$ be the labelled given by the expert of the i -th object. Our goal is to learn the weight vector, \mathbf{w} , which will allow the labelled anomalies to have a score higher than the score threshold corresponding to the user choice of τ , $\mathbf{w} : q_{\mathbf{H}_A} \geq q_\tau$.

Using a hinge loss defined as:

$$l(q, \mathbf{w}; z_i, y_i) = \begin{cases} 0 & \text{if } \mathbf{w} \cdot \mathbf{z}_i \geq q \text{ and } y_i = \text{anomaly} \\ 0 & \text{if } \mathbf{w} \cdot \mathbf{z}_i < q \text{ and } y_i = \text{normal} \\ q - \mathbf{w} \cdot \mathbf{z}_i & \text{if } \mathbf{w} \cdot \mathbf{z}_i < q \text{ and } y_i = \text{anomaly} \\ \mathbf{w} \cdot \mathbf{z}_i - q & \text{if } \mathbf{w} \cdot \mathbf{z}_i \geq q \text{ and } y_i = \text{normal} \end{cases} \quad (\text{A1})$$

the weights for each t iteration of the active learning loop can be found by solving

$$\begin{aligned}
\mathbf{w}^{(t)} &= \operatorname{argmin}_{\mathbf{w}} \left\{ \frac{1}{|\mathbf{H}_A|} \sum_{\mathbf{z}_i \in \mathbf{H}_A} l_{\mathbf{z}_\tau}^i{}^{(t-1)} + \frac{1}{|\mathbf{H}_N|} \sum_{\mathbf{z}_i \in \mathbf{H}_N} l_{\mathbf{z}_\tau}^i{}^{(t-1)} \right. \\
&+ \frac{1}{|\mathbf{H}_A|} \sum_{\mathbf{z}_i \in \mathbf{H}_A} l_{\mathbf{z}_\tau}^i{}^{(t-1)} + \frac{1}{|\mathbf{H}_N|} \sum_{\mathbf{z}_i \in \mathbf{H}_N} l_{\mathbf{z}_\tau}^i{}^{(t-1)} \\
&\left. + \|\mathbf{w} - \mathbf{w}_p\|^2 \right\}, \tag{A2}
\end{aligned}$$

where

$$l_{\mathbf{z}_\tau}^i{}^{(t-1)} \equiv l(\hat{q}_\tau(\mathbf{w}^{(t-1)}), \mathbf{w}; \mathbf{z}_i, y_i), \tag{A3}$$

$$l_{\mathbf{z}_\tau}^i \equiv l(\mathbf{z}_\tau^{(t-1)} \cdot \mathbf{w}, \mathbf{w}; \mathbf{z}_i, y_i), \tag{A4}$$

$$\mathbf{w}_p \equiv \left[\frac{1}{\sqrt{N_{\text{nodes}}}}, \dots, \frac{1}{\sqrt{N_{\text{nodes}}}} \right]^T, \tag{A5}$$

$\mathbf{z}_\tau^{(t-1)}$ marks the final leaf position for the object at the quantile anomaly score threshold for iteration $t-1$ and $\hat{q}_\tau(\mathbf{w}^{(t-1)})$ denotes its anomaly score⁵.

⁵ By definition, both quantities were calculated with $\mathbf{w} = \mathbf{w}^{(t-1)}$.

APPENDIX B: IDENTIFIED ANOMALIES

Table B1: Anomalies identified by IF and AAD algorithms.

SN name	α	δ	Type	z	References
Isolation forest					
SN2006kg	01:04:16.98	+00:46:08.9	AGN	0.230	Bassett et al. (2006) ; Östman et al. (2011)
SN2213-1745	22:13:39.97	-17:45:24.5	SLSN-R	2.046	Cooke et al. (2012)
SDSS-II SN 17789	01:29:16.13	+00:42:37.9	SLSN		Sako et al. (2018)
Gaia16aye	19:40:01.10	+30:07:53.4	ULENS, CV		Bakis et al. (2016) ; Wyrzykowski et al. (2016)
SN1000+0216	10:00:05.86	+02 16 23.6	SLSN-II	3.899	Cooke et al. (2012)
SN2013am	11:18:56.94	+13:03:50.0	LL IIP ^a	0.003	Nakano et al. (2013) ; Lisakov et al. (2018)
AAD					
Gaia16aye	19:40:01.10	+30:07:53.4	ULENS, CV		Bakis et al. (2016) ; Wyrzykowski et al. (2016)
SN2016fbo	01:01:35.54	+17:06:04.3	Ia ^b	0.030	Foley et al. (2018)
SDSS-II SN 18391	02:22:42.43	+00:25:05.0	?Unknown/?Star ^c		Sako et al. (2018)
LSQ13ccw	21:35:51.64	-18:32:52.0	Ibn	0.060	Pastorello et al. (2015)
SN2003gs	02:27:38.36	-01:09:35.4	Ia Pec	0.005	Krisciunas et al. (2009)
SN2006mr	03:22:42.84	-37:12:28.5	Ia-91bg	0.006	Contreras et al. (2010)
SN2007N	12:49:01.25	-09:27:10.2	Ia-91bg	0.013	Stritzinger et al. (2011) ; Folatelli et al. (2013)
SN2007ax	08:22:43.26	+22:33:16.9	Ia-91bg	0.007	Stritzinger et al. (2011) ; Folatelli et al. (2013)
SN2005dm	02:18:39.25	-06:54:10.8	Ia-91bg	0.017	Aldering et al. (2005) ; González-Gaitán et al. (2014)
SN2002fb	01:57:48.90	+36:20:26.3	Ia-91bg	0.016	Blondin et al. (2012)
PS1-12sk	08:44:54.86	+42:58:16.9	Ibn	0.054	Sanders et al. (2013)

^a LL IIP — low-luminosity IIP supernovae.^b LC in the Open Supernova Catalog has a bad quality and contains wrong photometrical points that make it looks anomalous.^c Unknown object in [Sako et al. \(2018\)](#); host classified as star by SDSS DR15.

APPENDIX C: LIGHT CURVES OF SELECTED ANOMALIES

This paper has been typeset from a $\text{\TeX}/\text{\LaTeX}$ file prepared by the author.

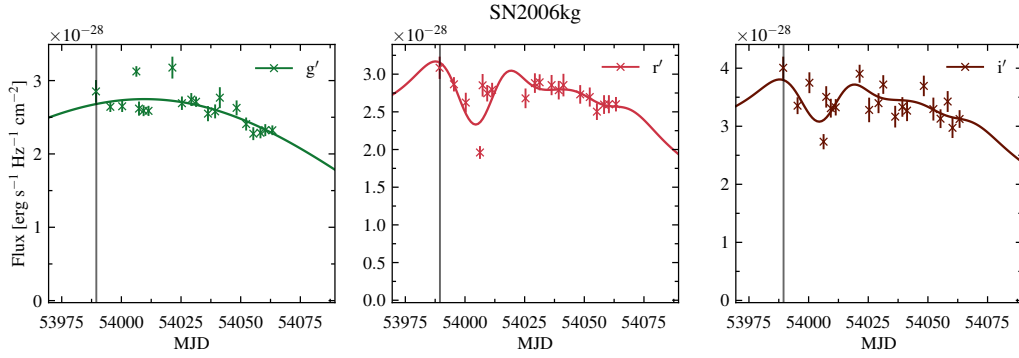


Figure C1. Light curves in $g'r'i'$ filters of active galactic nucleus SN2006kg (Sako et al. 2018). Solid lines are the results of our approximation by MULTIVARIATE GAUSSIAN PROCESS. The vertical line denotes the moment of maximum in r' filter.

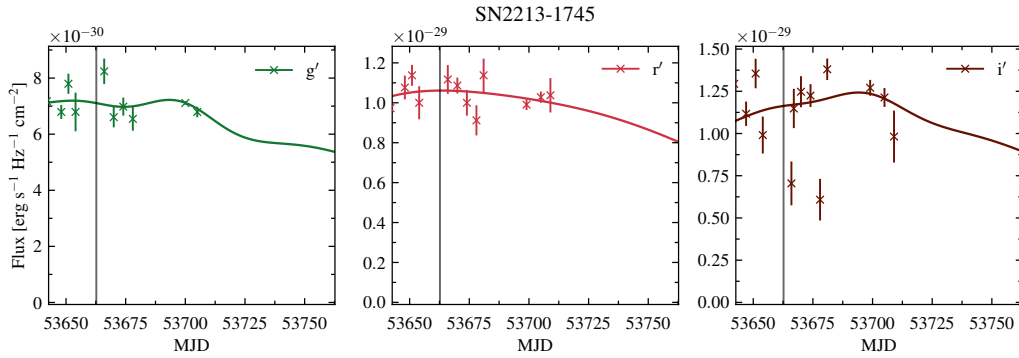


Figure C2. Light curves in $g'r'i'$ filters of super-luminous supernova 2213-1745 (Cooke et al. 2012). Solid lines are the results of our approximation by MULTIVARIATE GAUSSIAN PROCESS. The vertical line denotes the moment of maximum in r' filter.

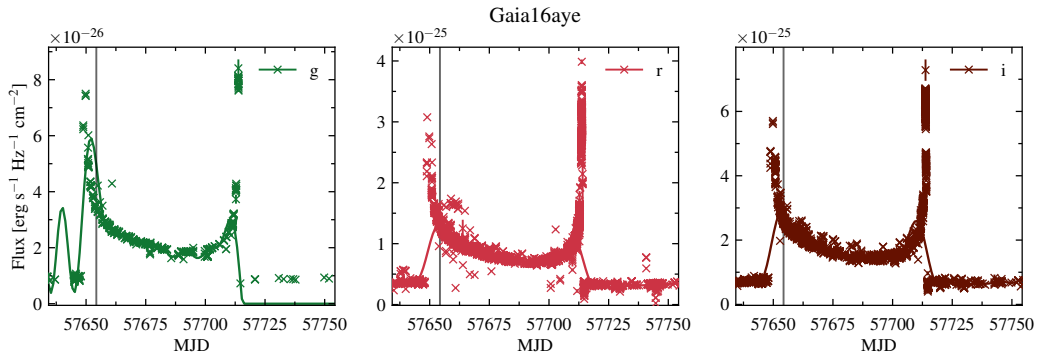


Figure C3. Light curves in gri filters of binary microlensing event Gaia16aye (<http://gsaweb.ast.cam.ac.uk/alerts/alert/Gaia16aye/followup>). Solid lines are the results of our approximation by MULTIVARIATE GAUSSIAN PROCESS. The vertical line denotes the moment of maximum in r filter.